Second-Order ab Initio Møller−Plesset Study of Optimum Chain Length for Total (Electronic Plus Vibrational) β(−ωσ;ω1,ω2) of a Prototype Push-Pull Polyene

ARTICLE *in* THE JOURNAL OF PHYSICAL CHEMISTRY A · JULY 2001

Impact Factor: 2.69 · DOI: 10.1021/jp011318w

Second-Order ab Initio Møller−Plesset Study of Optimum Chain Length for Total (Electronic Plus Vibrational) $\beta(-\omega_\sigma;\omega_1,\omega_2)$ of a Prototype Push-Pull Polyene

Denis Jacquemin,*[,†,||] Benoît Champagne,[†,⊥] Eric A. Perpète,[†,#] Josep M. Luis,[‡,§] and Bernard Kirtman[‡]

Laboratoire de Chimie Théorique Appliquée, Facultés Universitaires Notre-Dame de la Paix, 5000 Namur, Belgium, Department of Chemistry and Biochemistry, University of California, Santa Barbara, California, and Institute of Computational Chemistry and Department of Chemistry, University of Girona, Campus de Montilivi, 17071 Girona, Catalonia, Spain

Received: April 9, 2001; In Final Form: July 23, 2001

Static as well as dynamic electronic and vibrational longitudinal first hyperpolarizabilities (β_L^e and β_L^v) of α,*ω*,-nitro,amino-polyacetylene oligomers, containing up to 16 unit cells, have been computed at the Hartree−Fock and second-order Møller−Plesset levels using the 6-31G atomic basis set. The curve of first hyperpolarizability per unit cell versus the number of unit cells presents a maximum that defines the optimal chain length for NLO applications. Modifications in electronic structure occurring when electron correlation is included lead to an increase in the height of the maximum β_L^e by a factor of 2. A similar enhancement arises from the corresponding change in equilibrium geometry, which, in addition, shifts the position of the maximum toward longer chain lengths. Frequency dispersion also has a major effect on the position and magnitude of the optimal point. The contribution of the vibrational hyperpolarizability is relatively small when correlation and frequency dispersion are included. Our results are compared with experiment, as well as other calculations, and implications are drawn.

I. Introduction

During the past twenty years, numerous experimental and theoretical investigations have focused on determining the static and dynamic first hyperpolarizability, i.e., $\beta(0;0,0)$ and $\beta(-\omega_\sigma;\omega_1,\omega_2)$ of π-conjugated organic systems, which appear to be promising for nonlinear optical (NLO) applications. To design a molecule with a large β, one needs to effectively combine delocalization and asymmetry. A molecule possessing very delocalizable electrons will become highly polarized in an external electric field. This explains the large longitudinal third-order susceptibilities observed, for example, in *trans*-polyene chains. However, for molecules with an inversion center such as a *trans*-polyene, all odd-order hyperpolarizabilities vanish. To circumvent this problem, a common procedure is to make the chain asymmetric by substituting a strong electron donor at one end and a strong electron acceptor at the other. Although other strategies for building β molecules have been investigated,[1−12] these so-called push-pull conjugated molecules remain the most intensively studied class of second-order NLO compounds. Many possibilities exist by changing the donor, the acceptor, and the conjugated linker.[2]

An important optimizable parameter is the length of the conjugated linker. Consider the linker that will be examined here, namely a polyene chain containing *N* repeat units. In that case the figure of merit, which is essentially proportional to $\beta_L[N]/N$ (the subscript L indicates the longitudinal direction), must exhibit a maximum magnitude at some intermediate *N*. As discussed below, this follows on general grounds from the interplay between electron delocalization along the linker and the asymmetry at the chain ends.[6] Since the donor and the acceptor each have a finite range of interaction, the value of β_L will saturate for sufficiently large *N* and, hence, in that limit, $\beta_L[N]/N$ will approach zero. Such localized asymmetry has been nicely demonstrated by Tretiak, et al.[13] using density matrix plots. On the other hand, for small *N* the first-order nonlinear polarization of the linker by the donor and acceptor will grow supralinearly with *N* due to electron delocalization. This leads to an increase in the magnitude of $\beta_L[N]/N$ as *N* increases and, ultimately, to a maximum at intermediate *N* because of the competing decay from saturation as *N* becomes large. The occurrence of a maximum was first verified computationally by Morley and co-workers.[14] In addition to further work of the latter group,[15−17] subsequent studies dealing primarily with the chain length dependence have been carried out by Matsuzawa and Dixon,[18] Peng, et al.,[19] and Tretiak, et al.[13]

All of the calculations mentioned above were done by semiempirical methods, often by a procedure that is not fully size-consistent. Thus, an ab initio treatment is desirable in order to gain a reliable quantitative understanding of the factors that influence the position and magnitude of the maximum. In this regard it is imperative to include electron correlation (EC)[20,21] since it has a large effect. One possible method of calculation is density functional theory (DFT), but it has been shown that DFT using conventional XC potential is unsuitable for electrical properties of conjugated chains.[22] In addition to FCI, the most reliable EC method for structural studies is CCSD(T). In systems where CCSD(T) is impractical, as in the present case, the next

* Corresponding author.
† Facultés Universitaires Notre-Dame de la Paix.
‡ University of California.
§ University of Girona.
|| Postdoctoral Researcher of the Belgian National Fund for Scientific Research.
⊥ Senior Research Associate of the Belgian National Fund for Scientific Research.
Research Associate of the Belgian National Fund for Scientific Research.

10.1021/jp011318w CCC: $20.00
Published on Web 10/02/2001

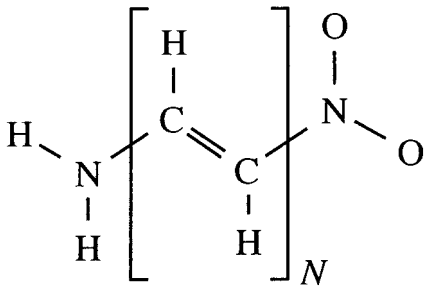

Figure 1. α, ω-nitro,amino polyacetylene oligomers; *N* is the number of unit cells.

best choice is second-order Møller−Plesset perturbation theory (MP2). It has been found empirically[23] that including corrections through fourth-order (MP4), more often than not, leads to divergence of electronic energies from the experimental value. A similar comprehensive investigation has not been undertaken for properties such as β. However, for an NH_2 donor and an NO_2 acceptor attached to small polyene linkers ($N = 1$, 2, and 3), it has been shown[21] that there is only a small difference in β between MP2 and MP4. In the same study the difference between either of these perturbation methods and CCSD(T) was found to be on the order of 5%, although the trend with N suggests more significant deviations [$\beta^{MP2} > \beta^{CCSD(T)}$] in longer chains. There is also evidence[24−28] from calculations on the second hyperpolarizability of butadiene that MP2 will somewhat overestimate the nonlinear polarization of the polyene linker. Nonetheless, MP2 appears sufficient to meet our twin goals of semiquantitative accuracy and computational feasibility for the system of interest in this paper.

In this first correlated ab initio study of the optimum chain length for β in a push-pull system, we have chosen to use as the prototype a polyene linker with an NH_2 donor and an NO_2 acceptor (Figure 1). In addition to EC, we also want to take into account the frequency dispersion of the electronic β. Fortunately, it has been demonstrated in ref 21 that multiplicative scaling of the Hartree−Fock (HF) dispersion, using the ratio of static HF and correlated values, will yield accurate frequency dependence for the push-pull polyenes considered here. So that is the procedure we will follow.

From many studies (see, for example, ref 29) it is now known that vibrational motions can make an important contribution to the frequency-dependent β in the optical region, particularly for the electrooptic Pockels effect (EOPE). This is primarily due to the nuclear relaxation (NR) term,[30,31] which arises from the shift in equilibrium geometry induced by the static electric field. There are also contributions[32] from zero-point vibrational averaging (ZPVA), as well as the effect of nuclear relaxation on the ZPVA. We will assume here that the latter two terms are negligible, in line with a recent investigation for the $N = 3$ compound.[32] Although correlated NR hyperpolarizabilities have been determined for small molecules,[33] systems of the size examined here have only been considered at the HF level.[11] However, such correlated calculations can now be carried out as the result of methodologies to be discussed in the following section.

A description of the computational techniques employed in this investigation is given in section II. Then, in section III, the results are presented and quantitatively analyzed for the effects of electron correlation, dispersion, and vibration in terms of localized chain-end asymmetry and delocalization along the linker. After a comparison with previous studies, the final section contains a summary and concluding remarks.

II. Methodology

The ground-state geometry of each oligomer was fully optimized using the 6-31G atomic basis set within the HF and MP2 schemes (frozen-core approach). This was achieved with the Gaussian 94 program,[34] under the condition that the residual forces are less than 10^{-5} au. The MP2/6-31G method provides a bond length alternation at the center of the chain of 0.07 Å for long oligomers, in reasonable agreement with the MP2/6-311G* value of 0.06 Å.[35] For the very long chains ($N = 15$ and 16), the MP2 optimization is computationally out of reach and the geometries were determined by extrapolating from shorter chains. A test revealed that the extrapolated and optimized $N = 14$ MP2 geometries are close enough so that the $\beta_L[N]/N$ value is affected by less than 1%. The same 6-31G basis was used to determine the NLO properties. For the substituted polyene chains, this basis set has been shown to be adequate in order to obtain reliable β values.[21] For example, the difference between the MP2/6-31G and MP2/auc-cc-pVDZ $\beta_L[N = 3]$ is smaller than 7%. In this paper, the usual convention for describing the method chosen, is used: "β calculation method//geometry optimization method".

The imposition of an electric field $\vec{F}$ on a molecule leads to a reorganization of its electronic charge distribution and, consequently, to a modification of its energy (E). Within the dipolar approximation, the modified charge distribution may be characterized by an induced dipole moment defined as

$$\Delta\mu_i = -\left(\frac{\partial E}{\partial F_i}\right) \tag{1}$$

where i is a Cartesian coordinate. If the induced dipole moment $\vec{\mu}$ is expanded as a Taylor series in $\vec{F}$, then

$$\Delta\mu_i(\omega_\sigma) = \mu_i(\omega_\sigma) - \mu_i^0\delta_{0,\omega\sigma} = \frac{1}{1!}\sum_j \alpha_{ij}(-\omega_\sigma;\omega_1)F_j(\omega_1) + \frac{1}{2!}K^{(2)}\sum_j\sum_k \beta_{ijk}(-\omega_\sigma;\omega_1,\omega_2)F_j(\omega_1)F_k(\omega_2) + \cdots \tag{2}$$

where $K^{(2)}$ ensures that the various $\beta(-\omega_\sigma;\omega_1,\omega_2)$ associated with different NLO processes converge toward the same static limit ($\beta(0;0,0)$). ω_1 and ω_2 are the circular frequencies of the incoming electric fields; ω_σ defines the circular frequency of the outgoing wave. Second harmonic generation (SHG), optical rectification (OR), and the electrooptic Pockels effect are denoted by $\beta(-2\omega;\omega,\omega)$, $\beta(0;\omega,-\omega)$, and $\beta(-\omega;\omega,0)$, respectively [$\beta_L(0;\omega,-\omega) = \beta_L(-\omega;\omega,0)$]. $\vec{\mu}^0$ is the dipole moment of the molecule in the absence of an external field and α_{ij} is a Cartesian component of the electric dipole polarizability tensor. Due to the large π-electron delocalization along the carbon backbone, the longitudinal component of the β tensor of α,ω-nitro,amino-PA chains (see Figure 1) dominates over all other components for oligomers longer than the tetramer, and we have restricted our study to that component $\beta_L(-\omega_\sigma;\omega_1,\omega_2)$.

The vibrational and electronic contributions to the hyperpolarizabilities can be separated by using the clamped nucleus approximation in which the motions of electrons and nuclei are treated sequentially rather than simultaneously.[36] As a consequence, the electronic properties are first computed for the nuclear configuration corresponding to the potential energy minimum and, then, nuclear motion on the ground-state electronic potential energy surface is taken into account.

A. Electronic First Hyperpolarizability. At the HF level $\beta_L^e(-\omega_\sigma;\omega_1,\omega_2)$ was calculated analytically by means of the

time-dependent Hartree−Fock (TDHF) procedure[37] implemented in the Hondo95.3 program.[38] In the static limit, the TDHF value agrees with the coupled perturbed Hartree−Fock (CPHF) result obtained from Gaussian94,[34] after changing the sign of the latter. The relation between $\beta_L^e(0;0,0)$ and $\beta_L^e(-\omega_\sigma;\omega_1,\omega_2)$ may be expressed as the power series expansion:[39−42]

$$\beta_L^e(-\omega_\sigma;\omega_1,\omega_2) = \beta_L^e(0;0,0)[1 + A\omega_L^2 + B\omega_L^4 + ...] \quad (3)$$

where

$$\omega_L^2 = \omega_\sigma^2 + \omega_1^2 + \omega_2^2 \quad (4)$$

$$\omega_L^4 = (\omega_L^2)^2 \quad (5)$$

For average and diagonal components, the parameters A and B do not depend on the optical process but are a function of the molecule treated and the method of calculation.[42] In this paper, we have determined A and B by a least-squares fit to the set of nine $\beta_L^e(-\omega;\omega,0)$ values for ($\omega = 0.00$; 0.05; ...; 0.40 au, (1 au = 455.63 Å^{-1}) using the function $[1 + A\omega_L^2 + B\omega_L^4 + \tilde{C}\omega_L^6]$, where $\tilde{C}$ is a linear combination of the C and C' of ref 42. This procedure typically gives an R value of 0.99999 with an estimated error on the order of 0.1% (2%) for A (B).

At the MP2 level of approximation $\beta_L(0;0,0)$ was evaluated by adopting the numerical finite field (FF) procedure:

$$\beta_L^{e;0,k}(0;0,0) = \lim_{F_L \to 0} \frac{E(-2^{k+1}F_L) - 2E(-2^kF_L) + 2E(2^kF_L) - E(2^{k+1}F_L)}{2(2^kF_L)^3} \quad (6)$$

where F_L was set equal to 2×10^{-4} a.u. (1 au of electric field = 5.1422 10^{11} Vm^{-1}) and the field amplitudes are given by 2^kF_L with $k = 0, 1, 2, ...$ 6. Starting with the above set of fields, one can systematically improve the accuracy on the estimated $\beta_L^e(0;0,0)$ by removing the high-order hyperpolarizability contaminations using the iterative Romberg formula:[43]

$$\beta_L^{e;p,k}(0;0,0) = \frac{4^p\beta_L^{e;p-1,k}(0;0,0) - \beta_L^{e;p-1,k+1}(0;0,0)}{4^p - 1} \quad (7)$$

where p is the order of the Romberg iteration. The FF calculations were realized with the Gaussian94 program[34] and, because of the frozen-core approximation, we were able to obtain the MP2 energy for molecules containing up to 16 unit cells. [It has been shown that the frozen-core approximation is accurate for the calculation of hyperpolarizabilities. See, for example ref 44.] During these evaluations the convergence criterion on the total energy was set to 10^{-13} a.u. A comparison of the FF/HF and CPHF $\beta_L(0;0,0)$ provides an estimate of the numerical accuracy attained by the FF/MP2 procedure. In our case, this difference was found to be smaller than 0.1%.

It was not computationally feasible for us to evaluate the correlated frequency-dependent hyperpolarizability $\beta_L^{e;EC}(-\omega_\sigma;\omega_1,\omega_2)$ directly for the extended systems of interest here. However, we could make an estimate by combining the static correlated $\beta^{e;EC}(0;0,0)$ with both the static and dynamic TDHF results, i.e., $\beta^{e;HF}(0;0,0)$ and $\beta^{e;HF}(-\omega_\sigma;\omega_1,\omega_2)$, according to the multiplicative approximation (sometimes referred to as the scaling correction),

$$\beta_L^{e;EC}(-\omega_\sigma;\omega_1,\omega_2) \approx \beta_L^{e;EC}(0;0,0)\frac{\beta_L^{e;HF}(-\omega_\sigma;\omega_1,\omega_2)}{\beta_L^{e;HF}(0;0,0)} \quad (8)$$

It has recently been demonstrated that this approximation is very good (errors smaller than 4%) for small ($N < 5$) α,ω-nitro,-amino-polyacetylene oligomers, even though $\beta_L^{e;HF}(0;0,0)$ and $\beta_L^{e;EC}(0;0,0)$ are quite different.[21] This behavior has been rationalized by showing that A^{HF} and A^{EC} of eq 3 are very similar.[21]

B. Vibrational First Hyperpolarizability. The vibrational first hyperpolarizability contributions were computed using the same 6-31G basis set as in the calculation of β^e. This basis has provided reliable values of nuclear relaxation hyperpolarizabilities for many conjugated systems.[11] For the β^v two different procedures were employed. At the HF level we adopted the double harmonic approximation $\beta^v(0;0,0) = [\mu\alpha]^{0,0}_{\omega=0}$, and the square bracket quantity on the right-hand side was evaluated directly using the well-known sum-over-modes perturbation formula[45] (for convenience we omit the subscript $\omega = 0$ from this point on). At the MP2 level a finite field nuclear relaxation treatment was carried out by means of the Bishop−Hasan−Kirtman (BHK) method.[46] The BHK method requires the electronic properties (μ^e, α^e, β^e, ...) at the field-free equilibrium geometry and at the relaxed equilibrium geometry in the presence of an external static electric field (the pump field). Consequently, the initial step is to reoptimize the geometry in the presence of an electric field, which must be done carefully so as to obey the Eckart conditions.[31] Then, the electric properties are obtained by numerical differentiation of the MP2 energy with respect to a so-called probe field, which leaves the geometry unaltered. The magnitude of the pump and probe fields utilized in our calculations is the same as given in section IIA.

If the field-free equlibrium geometry is denoted by R_0 and the pump-field-dependent geometry by R_F, it can be shown that

$$\mu^e(F, R_F) - \mu^e(0, R_0) = a_1F + \frac{1}{2!}b_1FF + ... \quad (9)$$

and

$$\alpha^e(F, R_F) - \alpha^e(0, R_0) = b_2F + ... \quad (10)$$

where

$$b_1 = \beta^e(0;0,0) + \beta^{NR}(0;0,0) \quad (11)$$

$$b_2 = \beta^e(0;0,0) + \beta^{NR}(-\omega;\omega,0)_{\omega\to\infty} \quad (12)$$

Here the superscript NR stands for the nuclear relaxation part of the vibrational hyperpolarizability. An analysis of the above approach[47,48] in the light of the Bishop and Kirtman perturbation treatment[45,49] leads to the following identities:

$$\beta^{NR}(0;0,0) = [\mu\alpha]^{0,0} + [\mu^3]^{1,0} + [\mu^3]^{0,1} \quad (13)$$

$$\beta^{NR}(-\omega;\omega,0)_{\omega\to\infty} = \frac{1}{3}[\mu\alpha]^{0,0} \quad (14)$$

$$\beta^{NR}(-2\omega;\omega,\omega)_{\omega\to\infty} = 0 \quad (15)$$

for the diagonal components as well as the isotropic averages. Except for contributions to the hyperpolarizability (ignored in this paper) that arise from the ZPVA (both directly and through nuclear relaxation),[32] β^{NR} includes all vibrational contributions that do not vanish in the infinite optical frequency limit. Since

TABLE 1: Chain Length Dependence of $\beta_L[N](0;0,0)$ Calculated for α,ω-nitro, Amino-PA Using the 6-31G Atomic Basis Set[a]

	HF geometry			MP2 geometry			
	electronic		vibrational	electronic		vibrational	
N	HF	MP2	$[\mu\alpha]^{0,0}$	HF	MP2	$[\mu\alpha]^{0,0}$	$[\mu^3]^{1,0}+[\mu^3]^{0,1}$
1	313.4	847	733	379.2	1096	778	51
2	1507.8	3661	3319	1798.1	4640	3198	336
3	4101.2	9554	8940	5008.9	12343	7994	761
4	8240.8	18504	17377	10500.4	24929	14633	1390
5	13563.3	29484	27310	18398.6	42086	21958	1906
6	19488.3	41131	37270	28447.9	62658	28531	2184
7	25430.0	52306	46284	40059.5	85064	34194	2273
8	31000.5	62465	53933	52558.0	107777	36483	
9	36001.5	71072	60204	65326.9	129606		
10	40371.7	78107	65194	77870.5	149775		
11	44124.3	84033	69080	89829.8	167833		
12	47315.8	88930	72036	100976.9	183683		
13	50012.0	92907	74213	111189.2	197334		
14	52283.5	96119		120429.2	208950		
15	54202.9	98778		128605.1	218684		
16	55810.5	100966		135813.0	226792		

[a] All results are in a.u.; N = number of CH=CH units.

the optical frequency used is ordinarily much larger than molecular vibrational frequencies, this infinite optical frequency approximation turns out to be quite accurate for typical optical frequencies whenever β^{NR} is important.[11] Numerical evaluation of the longitudinal b_1 and b_2, combined with knowledge of $\beta_L^e(0;0,0)$ at the equilibrium geometry, gives access to the static and ($\omega \rightarrow \infty$) dynamic β^{NR}. Since only the double harmonic term is required for the EOPE, our sum-over-mode HF calculations are sufficient in combination with eq 14 to yield that property, though not $\beta^{NR}(0;0,0)$.

III. Results and Discussion

A. Electronic First Hyperpolarizability. *1. Electron Correlation Effects.* The inclusion of EC affects the calculated NLO properties in two ways. On one hand, EC has a direct impact on the electronic structure of the compounds and thereby on β_L^e. On the other hand, when EC is included, the optimal ground-state geometry is modified, leading to an additional indirect change in β_L^e. The relative importance of the direct and indirect EC contributions to NLO properties depends on the system considered.[7,50,51] In the case of substituted PA chains, the bond length alternation (BLA), i.e., the difference between carbon−carbon single and double bond lengths, is considerably smaller in the MP2 equilibrium geometry than in the HF geometry. For example, the MP2/6-31G BLA at the center of the 14 unit cell compound is 0.072 Å, whereas the corresponding HF/6-31G value is 0.112 Å. Consequently, the geometry variation can be quite important as seen below.

Both direct and indirect effects were investigated for the entire set of compounds with the results shown in Table 1. The corresponding values per unit cell of $\beta_L^e[N](0;0,0)/N$, are displayed as a function of the chain length in Figure 2. All four curves have the same general shape: an initial fast increase; then a maximum; and, finally, a gradual falloff toward zero at the infinite chain limit. This peculiar shape originates from the interplay between asymmetry and delocalization as discussed further in section IIIC. The direct effect of EC is to multiply the height of the maximum by roughly a factor of 2 and shift its position slightly toward shorter chain length (for both

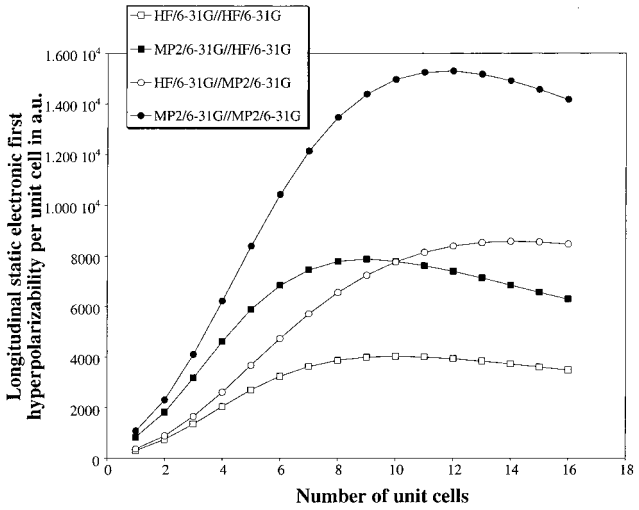

Figure 2. $\beta_L^e[N](0;0,0)/N$ obtained with the CPHF and FF-MP2 methods at the HF and MP2 equilibrium geometries. All calculations were carried out using the 6-31G basis set.

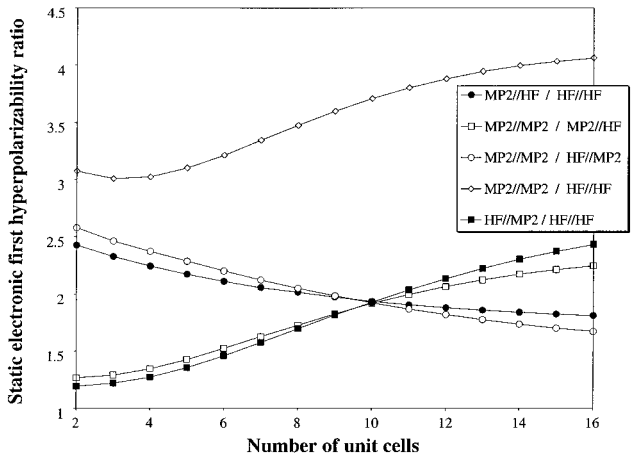

Figure 3. Evolution with chain length of various ratios reflecting the direct and indirect effects of EC on the electronic first hyperpolarizability.

geometries). A similar factor of 2 enhancement has been found in *p*-nitroaniline.[52] The indirect effect of EC is very important as well. It moves the position of the maximum toward longer chain length (from $N = 10(9)$ to $N = 14(12)$ for the HF(MP2) property calculation) and roughly doubles the height of $\beta_L^e[N](0;0,0)/N$ at the maximum. This behavior is a consequence of the smaller BLA in the MP2 geometry, which increases the conjugation length and allows the two end groups to interact more strongly. The combination of the direct and indirect effects of EC at the MP2 level increases the maximum $\beta_L^e[N](0;0,0)/N$ by almost a factor of 4 and alters its location from $N = 10$ to $N = 12$.

It is of interest from a practical[7,50,51] and theoretical point of view to compare the chain length dependence of the MP2 and HF hyperpolarizabilities calculated at either the HF or MP2 geometry. Figure 3 displays the evolution with N of several relevant ratios. Note that the direct impact of EC (either MP2//HF/HF//HF or MP2//MP2/HF//MP2) decreases monotonically with N, whereas the indirect impact (either HF//MP2/HF//HF or MP2//MP2/MP2//HF) increases monotonically. It is striking that the direct contribution does not depend significantly on the geometry (open versus filled circles). Likewise the indirect contribution is insensitive to the method of evaluation (open versus filled squares).

TABLE 2: $\beta^e_L[N](-\omega_\sigma;\omega_1,\omega_2)$ of α,ω-nitro, Amino-polyacetylene Chains in a.u.[a]

	$\lambda = 632.8$ nm	$\lambda = 1064.0$ nm	$\lambda = 1907.0$ nm	
N	EOPE/OR	EOPE/OR	EOPE/OR	SHG
1	514.5	420.6	391.5	417.7
2	2705.4	2059.4	1838.0	2040.5
3	8469.1	5943.1	5274.9	5874.1
4	20025.6	12906.5	11172.9	12725.1
5	39492.8	23382.7	19766.9	22999.5
6	68328.4	37278.0	30833.3	36587.5
7	106880.6	53961.1	43758.7	52857.4
8	154540.9	72564.3	57812.2	70954.9
9	209991.1	92184.1	72296.4	89998.7
10	271598.0	112030.9	86642.1	109223.4
11	337587.0	131473.7	100427.2	128021.7
12	406225.2	150032.8	113350.5	145934.9
13	475998.8	167417.0	125257.9	162687.9
14	545887.6	183514.6	136115.6	178178.7
15	613409.7	197970.4	145733.2	192072.0
16	678659.0	211001.3	154294.8	204581.4

[a] All results were obtained using the TDHF/6-31G procedure at the MP2/6-31G ground state geometry. SHG stands for second-harmonic generation $\beta^e_L[N](-2\omega;\omega,\omega)$; EOPE for the electrooptic pockels effect $\beta^e_L(-\omega;\omega,0)$; and OR = EOPE for optical rectification $\beta^e_L[N](0;\omega,-\omega)$.

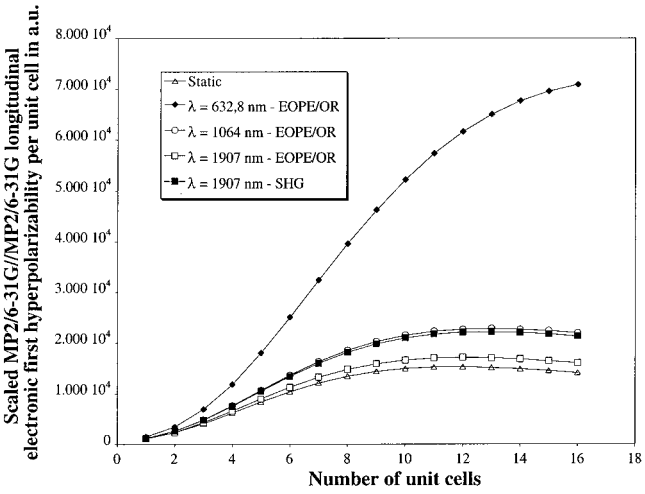

Figure 4. Evolution of MP2/6-31G//MP2/6-31G $\beta^e_L[N](-\omega_\sigma;\omega_1,\omega_2)/N$ with *N* for different frequencies and NLO processes. The multiplicative procedure (eq 8) was used to obtain the frequency-dependence displayed in this graph.

2. Frequency Dispersion Effects. Table 2 gives the $\beta^e_L[N](-\omega_\sigma;\omega_1,\omega_2)$calculated at the MP2/6-31G geometry using the TDHF/6-31G procedure for three common laser frequencies. The corresponding EC values per unit cell, estimated by means of eq 8, are given in Figure 4 and the results of fitting to eq 3 are given in Table 3. Due to the small first excitation energy of large chains, it was not possible to evaluate the $\beta^e_L[N](-2\omega;\omega,\omega)$ at wavelengths of 632.8 and 1064.0 nm.

As can be seen in Figure 4, the frequencies of the external electric fields and the type of NLO process have a large effect on the chain-length dependence. Decreasing the wavelength of the fields shifts the position of the maximum toward longer chain length and increases its height. For $\lambda = 632.8$ nm (1064 nm), the position of the EOPE MP2/6-31G//MP2/6-31G maximum is displaced from the static value of $N = 12$ to $N \geq 16$ ($N = 13$), and its amplitude is multiplied by a factor ~4.5 (1.5). Thus, lowering λ has the same general consequence as decreasing the BLA. The curves obtained for $\beta^e_L[N](-2\omega;\omega,\omega)$ (with $\lambda =$ 1907.0 nm) and $\beta^e_L[N](-\omega;\omega,0)$ (with $\lambda = 1064.0$ nm) are extremely close to one another because the value of ω_L^2 (cf. eq 4) corresponding to these two situations is very similar (~3.5 10^{-3} a.u.).

TABLE 3: Values of *A* and *B* Obtained by Fitting $\beta^e_L[N](-\omega;\omega, 0)$ versus ω_L^2 as in Equation 3 (see the text for more details)[a]

N	static	A	*B*/100
1	379.2	27.6	6
2	1798.1	35.8	9
3	5008.9	45.0	13
4	10500.4	53.6	21
5	18398.6	61.8	28
6	28447.9	69.2	35
7	40059.5	75.8	41
8	52558.0	81.7	47
9	65326.9	86.8	53
10	77870.5	91.3	58
11	89829.8	95.2	64
12	100976.9	98.7	67

[a] All results were obtained by the TDHF/6-31G//MP2/6-31G method.

The *A* and *B* coefficients of Table 3 converge with chain length much slower than do those corresponding, for example, to the electric-field-induced second-harmonic generation (EFISHG) of polysilane oligomers.[53] Due to the slow convergence, they are not useful for predicting $\beta^e_L[N](-\omega_\sigma;\omega_1,\omega_2)$ when $N \geq 13$ but are helpful for estimating $\beta^e_L[N](-\omega_\sigma;\omega_1,\omega_2)$ of $N \leq 12$ compounds at frequencies not listed in Table 4, provided that higher-order terms in eq 3 can be neglected (for $N = 12$ using the criterion $A > 10B\omega_L^2$, this condition is met when $\omega_L < \sim 0.038$ au; this corresponds to $\lambda^{EOPE} = 1700$ nm and $\lambda^{SHG} = 2940$ nm).

B. Vibrational First Hyperpolarizability. In Table 1 we have listed the vibrational/nuclear relaxation contributions to the first hyperpolarizability of α,ω-nitro,amino-PA oligomers. These contributions were computed following the procedures described in section IIB.

If one focuses on the HF results, it can be seen from Table 1 and Figure 5 that, for the same *N*, $[\mu\alpha]^{0,0}$ is larger than $\beta^e_L(0;0,0)$ by a factor varying roughly from 2.0 for the shortest chains to 1.5 for the longest. This leads to a more pronounced bell-shaped behavior for the vibrational (as compared to the electronic) property per unit cell and a maximum at smaller *N*. Figure 6 illustrates how $[\mu\alpha]^{0,0}$ decreases when one steps to the MP2 level. The effect is larger for longer chains; thus the ratio $[\mu\alpha]^{0,0}_{MP2}/[\mu\alpha]^{0,0}_{HF}$ diminishes from 0.96 to 0.71 upon going from the dimer to the octamer. This leads to the maximum in $[\mu\alpha]^{0,0}/N$ occurring at shorter chain lengths ($N = 7$ for MP2 versus $N = 8$ for HF). At the same time the electronic β is increased by EC so that the $[\mu\alpha]^{0,0}/\beta^e$ ratio becomes substantially less than unity; this ratio is 0.42, for example, at $N = 7$.

The first-order electrical and mechanical anharmonic contributions to the correlated (MP2) β^{NR} are small with respect to the corresponding $[\mu\alpha]^{0,0}$. Indeed, the $[\mu^3]^I/[\mu\alpha]^{0,0}$ ($[\mu^3]^I = [\mu^3]^{1,0} + [\mu^3]^{0,1}$) ratio is 0.1 for the dimer and goes down to 0.07 for the longest system investigated. Thus, at the MP2 level, anharmonicity does not significantly affect $\beta^{NR}_L[N](0;0,0)$ nor the sum $\beta^e_L[N](0;0,0) + \beta^{NR}_L[N](0;0,0)$. For the OR/EOPE processes, only the doubly harmonic term is present. It appears in eq 14 with a coefficient of 1/3, which makes its contribution to the MP2 first hyperpolarizability quite small.

C. Analysis of Trends in Chain Length Evolution. To obtain a detailed analysis for the effects of EC on the electronic

TABLE 4: Parameters Obtained by Least-Square Fits to the Functional Form for $\beta_L[N]/N$ Given by Equation 16[a]

method	β_L	m_1	m_2	m_3	m_4
HF/6-31G//HF/6-31G	$\beta_L^e(0;0,0)$	24618	29840	6.92	4.76
MP2/6-31G//HF/6-31G	$\beta_L^e(0;0,0)$	43382	55731	6.27	4.75
HF/6-31G//MP2/6-31G	$\beta_L^e(0;0,0)$	63720	68263	8.82	4.57
MP2/6-31G//MP2/6-31G	$\beta_L^e(0;0,0)$	102826	110329	7.71	4.09
MP2/6-31G//MP2/6-31G	$\beta_L^e(-\omega;0,\omega)$ $\lambda = 632.8$ nm	531091	540768	9.83	4.00
MP2/6-31G//MP2/6-31G	$\beta_L^e(-\omega;0,\omega)$ $\lambda = 1064.0$ nm	166195	183956	8.50	4.80
MP2/6-31G//MP2/6-31G	$\beta_L^e(-\omega;0,\omega)$ $\lambda = 1907.0$ nm	120712	138724	8.11	5.03
MP2/6-31G//MP2/6-31G	$\beta_L^e(-2\omega;\omega,\omega)$ $\lambda = 1907.0$ nm	160387	176835	8.43	4.72
HF/6-31G//HF/6-31G	$[\mu\alpha]_L^{0,0};\omega = 0$	29567	55426	5.27	6.21
MP2/6-31G//MP2/6-31G	$[\mu\alpha]_L^{0,0};\omega = 0$	18735	52246	4.61	8.39

[a] m_1 and m_2 have dimensions of first hyperpolarizability and are expressed in a.u.; m_3 and m_4 are dimensionless.

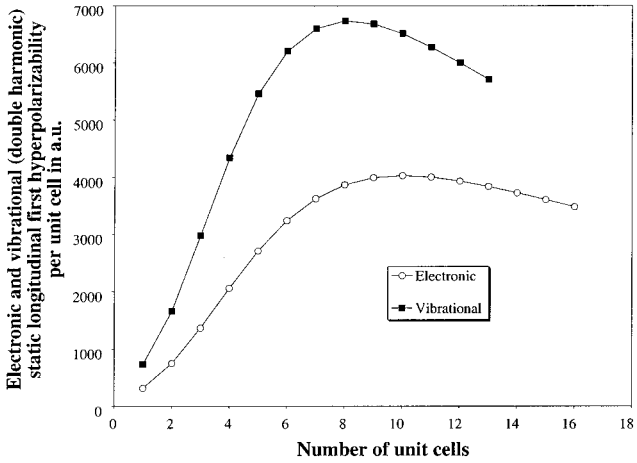

Figure 5. Comparison between $\beta_L^e[N](0;0,0)/N$ and double harmonic $\beta_L^{NR}[N](0;0,0)/N$ obtained at the HF/6-31G//HF/6-31G level.

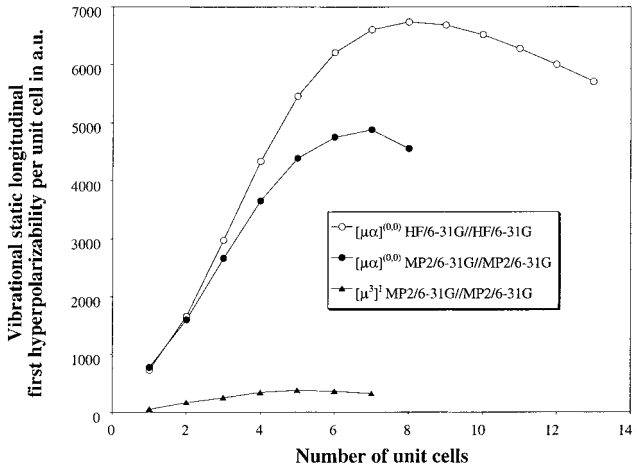

Figure 6. Nuclear relaxation $\beta_L^{NR}[N](0;0,0)/N$ contributions obtained at different levels of approximation.

and vibrational contributions to $\beta_L[N]/N$ versus N, we fit the data to[6,7,54]

$$\beta_L[N]N = \left[m_1 + m_2 \tanh\left(\frac{N - m_3}{m_4}\right)\right]\left(\frac{1}{N}\right) \qquad (16)$$

In eq 16, the initial supralinear growth with N is governed by the "tanh" term on the right-hand side. The amplitude of this growth term is m_2 while m_3, m_4 determine its shape. In fact, m_3 is the inflection point and $1/m_4$ is the saturation rate parameter. Since all the $\beta_L[N]$ curves that are to be fit extrapolate (formally) to zero at $N = 0$, m_1 is just the negative of the delocalization term evaluated at $N = 0$. Although the above fitting function does incorporate the basic physics, we emphasize that it does not give quantitative accuracy and is employed here only to interpret trends.

We have used a least-squares fitting procedure, including all chain lengths from $N = 2$ to the largest oligomer treated, to obtain the m_j coefficients in eq 16. The results are displayed in Table 4. For the static β_L^e, the indirect effect of EC substantially increases the electronic susceptibility of the linker (cf. m_2). This was expected because the decrease in BLA produces greater electron delocalization. The direct effect of EC yields a change in the same direction and of roughly the same magnitude, though somewhat smaller. On the other hand, there is an opposite effect on the inflection point (cf. m_3) in the two cases; the direct effect results in a decrease whereas the geometry change produces an increase. Thus, the change in electronic structure due to EC tends to decrease the conjugation length while at the same time increasing the interaction between the chain ends. It is interesting to note that both EC effects are consistent with the behavior found[50] for the second electronic hyperpolarizability (rather than the linear polarizability) of polyene chains.

Upon including frequency dispersion, the amplitude of m_2, again according to expectation, increases along with $1/\lambda$. The static double harmonic vibrational term, however, behaves very differently from β_L^e. For the former only the sum of the direct and indirect EC effects is meaningful. The overall result of EC is to decrease m_1 and leave m_2 essentially unchanged. This mimics the behavior of the linear electronic polarizability of the linker.[50] Perhaps the difference between the vibrational and electronic susceptibility is not too surprising when one considers that vibrational hyperpolarizabilities arise from lower-order terms in the dipole moment expansion of eq 2. Finally, for the vibrational component, the change in m_3 and m_4 due to EC is opposite to the change for the electronic component, further indicating that the vibrational and electronic β must be rationalized in different ways.

D. Comparisons with Other Theoretical and Experimental Results. Table 5 presents different theoretical electronic first hyperpolarizabilities evaluated for substituted PA chains. For purposes of comparison with other calculations and experiment $\beta_L^v[N]$ is not included although it is important for the static case. We report the maximum in $\beta_L^e[N]$ divided by the molecular weight (W). It is important to stress the difficulty in making comparisons because different authors choose different definitions for the first hyperpolarizability (longitudinal, vector, or intrinsic $\beta^e[N]$); use different methodologies (ab initio or semiempirical techniques with or without electron correlation); different geometries (optimized, ideal, or taken from crystallographic data); and different substituents. Nevertheless, the

TABLE 5: Maximum Electronic First Hyperpolarizabilities Per Unit Weight $[\beta^e/W]_{max}$ for Donor/Acceptor Substituted Polyenes Obtained by Various Methods[a]

β	method	chains ends	N_{max}	$[\beta^e/W]_{max}$	ref
static	MP2/6-31G//MP2/6-31G	NH_2/NO_2	13	4.3	
SHG, $\lambda = 1907.0$ nm	MP2/6-31G//MP2/6-31G	NH_2/NO_2	14	6.3	
EOPE, $\lambda = 1907.0$ nm	MP2/6-31G//MP2/6-31G	NH_2/NO_2	13	4.8	
EOPE, $\lambda = 1064.0$ nm	MP2/6-31G//MP2/6-31G	NH_2/NO_2	14	6.5	
EOPE, $\lambda = 632.8$ nm	MP2/6-31G//MP2/6-31G	NH_2/NO_2	≥ 16	19.2	
SHG, $\lambda = 1907$ nm	CNDOVSB−CIS//crystal	NMe_2/NO_2	≥ 24	236.4	15
SHG, $\lambda = 1907$ nm	CNDOVSB−CISD//crystal	NMe_2/NO_2	≥ 16	23.8	15
static	CNDOVSB−CIS//AM1	NMe_2/NO_2	12	0.8	16
static	AM1//AM1	NMe_2/NO_2	12	1.0	65
SHG, $\lambda = 1907$ nm	CNDOVSB−CIS//AM1	NMe_2/NO_2	≥ 18	2.1	16
static	PM3//PM3	Ph-NMe_2/NO_2	9	0.3	18
static	ZINDO//AM1	Ph-$NMe_2/(CN)_2$	10	1.3	13

[a] All hyperpolarizabilities are given in 10^{-30} cm^5 esu^{-1} g^{-1} mol. N_{max} is the number of unit cells corresponding to the maximum. In cases where the maximum was not determined, the largest value found is reported. For the ZINDO//AM1 calculation they were estimated from the graph provided by Tretiak and co-workers.[13]

estimated value of the optimal chain length for the static response is, in each case, between 9 and 13 unit cells. Moreover, it is very clear from the $\beta^e_L[N]$ reported by Morley and ourselves that frequency dispersion moves the position of the maximum toward longer chain length and strongly increases the optimal NLO response.

Only a few experiments provide numerical values for hyperpolarizabilities of compounds containing oligomeric linkers with a variable number of unit cells.[55,56] We can compare our $\beta^e_L[N]$ for the three smallest oligomers to the corresponding numbers reported by Alain and co-workers,[56] who have used EFISH measurements to evaluate SHG first hyperpolarizabilities. In accord with the treatment given here, we assume that the vibrational contribution is negligible. Then our calculated MP2/6-31G//MP2/6-31G $\beta^e_L[N](-2\omega;\omega,\omega)/W(\lambda = 1907$ nm) results, which are 0.11 ($N = 1$), 0.40 ($N = 2$), and 0.89 ($N = 3$) 10^{-30} cm^5 esu^{-1} g^{-1} mol (1 au of $\beta = 8.641\ 10^{-30}$ cm^5 esu^{-1}) may be compared directly to the experimental values of 0.07 ($N = 1$), 0.42 ($N = 2$), and 0.85 ($N = 3$) 10^{-30} cm^5 esu^{-1} g^{-1} mol. We want to stress that such very good agreement is fortuitous. Indeed, the measurements were realized in solution and the experimental push-pull groups are much larger than the nitro and amino groups used in this paper. Nevertheless, this comparison tends to show that the estimated theoretical evolution of $\beta^e[N]$ with N is meaningful.

The optimal calculated MP2/6-31G//MP2/6-31G $[\beta_L(0;0,0)/W]_{max}$ for substituted PA chains (4.3 10^{-30} cm^5 esu^{-1} g^{-1} mol) is very similar to that obtained for PMI[7] (4.2 10^{-30} cm^5 esu^{-1} g^{-1} mol). Both systems present reponses comparable to or even larger than the "best" push-pull molecules used in experiment because it is difficult to synthesize long conjugated chains that are both stereoregular and stable.

IV. Conclusions and Outlook

We have investigated the evolution with chain length of the longitudinal electronic and vibrational (nuclear relaxation = NR) first hyperpolarizabilities of donor/acceptor = NH_2/NO_2 substituted PA chains taking into account electron correlation, frequency dispersion, and anharmonic contributions to the NR hyperpolarizability. The $\beta_L[N]/N$ versus N curve must exhibit a maximum because of the interplay between delocalization and asymmetry. For short chains the asymmetric ends are connected and delocalization leads to a rapid initial increase, whereas for long chains the asymmetry is localized to the chain ends so that $\beta_L[N]/N$ approaches zero. Thus, there is an optimal linker length for the nonlinear response, which we have determined semiquantitatively.

It has been demonstrated that the inclusion of EC displaces the position of the maximum toward longer chain length and increases the optimal $\beta^e_L[N]$ value by a factor of 4. On the other hand, EC strongly decreases the relative static vibrational nuclear relaxation contribution. The latter is on the order of 1/3 the static electronic response at $N = 8$. A reduction by an additional factor of 3 occurs for OR/EOPE at typical optical frequencies. Both the position and height of the maximum are strongly affected by the frequency of the external electric fields. The shorter the wavelength, the larger the optimal response.

Although an initial comparison with experiment shows that the observed trend is similar to what we have obtained, the effects of the medium remain to be treated. Indeed, it has been shown that interactions between the molecule and the surroundings can substantially tune NLO responses.[57−64]

Acknowledgment. D.J., B.C., and E.P. thank the Belgian National Fund for Scientific Research for their Postdoctoral Researcher, Senior Research Associate, and Research Associate positions, respectively. They are indebted to Prof. J. M. André for his continuous support. J.M.L. acknowledges the financial assistance provided by the Generalitat de Catalunya through a Gaspar de Portolá grant. All calculations were performed on the IBM RS6000 cluster of the Namur Scientific Computing Facility (Namur-SCF). The authors gratefully acknowledge the financial support of the FNRS−FRFC, the 'Loterie Nationale' for the convention No. 2.4519.97, and the Belgian National Interuniversity Research Program on 'Sciences of Interfacial and Mesoscopic Structures' (PAI/IUAP No. P4/10).

References and Notes

(1) Clays, K.; Hendrickx, E.; Triest, M.; Verbiest, T.; Persoons, A.; Dehu, C.; Brédas, J. L. *Science* **1993**, *262*, 1419.

(2) Kanis, D. R.; Ratner, M. A.; Marks, T. J. *Chem. Rev.* **1994**, *94*, 195.

(3) Meyers, F.; Marder, S.; Pierce, B. M.; Brédas, J. L. *J. Am. Chem. Soc.* **1994**, *116*, 10703.

(4) Albert, I. D. L.; Marks, T. J.; Ratner, M. A. *J. Phys. Chem.* **1996**, *100*, 9714.

(5) Pan, F.; Wong, M. S.; Gramlich, V.; Bosshard, C.; Günter, P. *J. Am. Chem. Soc.* **1996**, *118*, 6315.

(6) Jacquemin, D.; Champagne, B.; Kirtman, B. *J. Chem. Phys.* **1997**, *107*, 5076.

(7) Jacquemin, D.; Champagne, B.; André, J. M. *Chem. Phys. Lett.* **1998**, *284*, 24.

(8) Verbiest, T.; Van Elshocht, S.; Kauranen, M.; Hellemans, M.; Sauwaert, J.; Nuckolls, C. N.; Kayz, T. J.; Persoons, A. *Science* **1998**, *282*, 913.

(9) Morley, J. O.; Hutchings, M. G.; Hall, N. *J. Phys. Chem. A* **1998**, *102*, 5802.

(10) Zyss, J.; Brasselet, S.; Thalladi, V. R.; Desiraju, G. R. *J. Chem. Phys.* **1998**, *109*, 658.
(11) Champagne, B.; Kirtman, B. Theoretical Aspects of Conjugated Organic Molecules and Polymers for NLO Devices in *Handbook of Advanced Electronic and Photonic Materials*; Nalwa, H. S., Ed.; Academic: San Diego, 2001; Vol. 9, Chapter 2, pp 63−126.
(12) Clays, K.; Persoons, A. Hyper-Rayleigh Scattering: Opportunities for Molecular, Supramolecular, and Device Characterization by Incoherent Second-Order Nonlinear Light Scattering in *Handbook of Advanced Electronic and Photonic Materials*; Nalwa, H. S., Ed.; Academic: San Diego, 2001; Vol 9, Chapter 5, p 229.
(13) Tretiak, S.; Chernyak, V.; Mukamel, S. *Chem. Phys. Lett.* **1998**, *287*, 75.
(14) Morley, J. O.; Docherty, V. J.; Pugh, D. *J. Chem. Soc., Perkin Trans. 2* **1987**, 1351.
(15) Albert, I. D. L.; Pugh, D.; Morley, J. O. *J. Chem. Soc., Faraday Trans.* **1994**, *90*, 2617.
(16) Morley, J. O. *J. Phys. Chem.* **1995**, *99*, 10166.
(17) Albert, I. D. L.; Morley, J. O.; Pugh, D. *J. Phys. Chem. A* **1997**, *101*, 1763.
(18) Matsuzawa, N.; Dixon, D. A. *Int. J. Quantum Chem.* **1992**, *44*, 497.
(19) Peng, W.; Peiwang, Z.; Chuanguang, W.; Cheng, Y. *J. Mol. Struct. (THEOCHEM)* **1999**, *459*, 155.
(20) Jacquemin, D.; Champagne, B.; André, J. M. *Int. J. Quantum Chem.* **1997**, *65*, 679.
(21) Jacquemin, D.; Champagne, B.; Hättig, C. *Chem. Phys. Lett.* **2000**, *319*, 327.
(22) Champagne, B.; Perpète, E.; Jacquemin, D.; Van Gisbergen, S.; Baerends, E.; Soubra-Ghaoui, C.; Robins, K.; Kirtman, B. *J. Phys. Chem. A* **2000**, *104*, 4755.
(23) Dunning, T. H.; Peterson, K. A.; Woon, D. E.; Van Mourik, T.; Wilson, A. K. 10th American Conference on Theoretical Chemistry, Boulder, Colorado, June 27-July 2 (Absracts, p 9).
(24) Maroulis, G. *J. Phys. Chem.* **1999**, *111*, 583.
(25) Rozyczko, P. B.; Bartlett, R. J. *J. Chem. Phys.* **1998**, *108*, 7988.
(26) Kirtman, B.; Toto, J. L.; Breneman, C.; De Melo, C. P.; Bishop, D. M. *J. Chem. Phys.* **1998**, *108*, 4355.
(27) Norman, P.; Luo, Y.; Jonsson, D.; Agren, H. *J. Chem. Phys.* **1997**, *106*, 1827.
(28) Norman, P.; Luo, Y.; Jonsson, D.; Agren, H. *J. Chem. Phys.* **1998**, *108*, 4355.
(29) Champagne, B.; Kirtman, B. *Chem. Phys.* **1999**, *245*, 213.
(30) Kirtman, B.; Champagne, B.; Bishop, D. *J. Am. Chem. Soc.* **2000**, *122*, 8007.
(31) Luis, J. M.; Duran, M.; Andrés, J.; Champagne, B.; Kirtman, B. *J. Chem. Phys.* **1999**, *111*, 875.
(32) Luis, J. M.; Champagne, B.; Kirtman, B. *Int. J. Quantum Chem.* **2000**, *80*, 471.
(33) Quinet, O.; Champagne, B. *Int. J. Quantum Chem.* **2000**, *80*, 871.
(34) Frisch, M. J.; Trucks, G. W.; Schlegel, H. B.; Gill, P. M. W.; Johnson, B. G.; Robb, M. A.; Cheeseman, J. R.; Keith, T.; Petersson, G. A.; Montgomery, J. A.; Raghavachari, K.; Al-Laham, M. A.; Zakrzewski, V. G.; Ortiz, J. V.; Foresman, J. B.; Cioslowski, J.; Stefanov, B. B.; Nanayakkara, A.; Challacombe, M.; Peng, C. Y.; Ayala, P. Y.; Chen, W.; Wong, M. W.; Andres, J. L.; Replogle, E. S.; Gomperts, R.; Martin, R. L.; F. D. J.; Binkley, J. S.; Defrees, D. J.; Baker, J.; Stewart, J. P.; Head-Gordon, M.; Gonzalez, C.; Pople, J. A. *GAUSSIAN 94*, revision B.1; Gaussian Inc.: Pittsburgh, PA, 1995.
(35) Perpète, E.; Champagne, B. *J. Mol. Struct. (THEOCHEM)* **1999**, *487*, 39.
(36) Bishop, D. M.; Kirtman, B.; Champagne, B. *J. Chem. Phys.* **1997**, *107*, 5780.
(37) Karna, S. P.; Dupuis, M. *J. Comput. Chem.* **1991**, *12*, 487.
(38) Dupuis, M.; Marquez, A.; Davidson, E. R. HONDO 95.3 from CHEM-Station, IBM Corporation, Neighborhood Road, Kingston, NY. 12401, 1995.
(39) Bishop, D. M. *J. Chem. Phys.* **1991**, *95*, 5489.
(40) Bishop, D. M.; De Kee, D. W. *J. Chem. Phys.* **1996**, *104*, 9876.
(41) Bishop, D. M.; De Kee, D. W. *J. Chem. Phys.* **1996**, *105*, 8247.
(42) Hättig, C. *Mol. Phys.* **1998**, *94*, 455.
(43) Rutihauser, H. *Numer. Matematik* **1963**, *5*, 48.
(44) Jacquemin, D.; Champagne, B.; André, J. M. *J. Mol. Struct. (THEOCHEM)* **1998**, *425*, 69.
(45) Bishop, D. M.; Kirtman, B. *J. Chem. Phys.* **1991**, *95*, 2646.
(46) Bishop, D. M.; Hasan, M.; Kirtman, B. *J. Chem. Phys.* **1995**, *103*, 4157.
(47) Bishop, D. M.; Dalskov, E. K. *J. Chem. Phys.* **1996**, *104*, 1004.
(48) Kirtman, B.; Champagne, B.; André, J. M. *J. Chem. Phys.* **1996**, *104*, 4125.
(49) Bishop, D. M.; Kirtman, B. *J. Chem. Phys.* **1998**, *109*, 9674.
(50) Toto, T. T.; Toto, J. L.; De Melo, C. P.; Hasan, M.; Kirtman, B. *Chem. Phys. Lett.* **1995**, *244*, 59.
(51) Toto, J. L.; Toto, T. T.; De Melo, C. P. *Chem. Phys. Lett.* **1995**, *245*, 660.
(52) Sim, F.; Chin, S.; Dupuis, M.; Rice, J. E. *J. Phys. Chem.* **1993**, *97*, 1158.
(53) Champagne, B.; Perpète, E.; André, J. M. *Int. J. Quantum Chem.* **1998**, *70*, 751.
(54) Champagne, B.; Jacquemin, D.; André, J. M.; Kirtman, B. *J. Phys. Chem. A* **1997**, *101*, 3158.
(55) Blanchard-Desce, M.; Runser, C.; Fort, A.; Barzoukas, M.; Lehn, J. M.; Bloy, V.; Alain, V. *Chem. Phys.* **1995**, *199*, 253.
(56) Alain, V.; Blanchard-desce, M.; Chen, C.; Marder, S. R.; Fort, A.; Barzoukas, M. *Synth. Met.* **1996**, *81*, 133.
(57) Champagne, B.; Mennucci, B.; Cossi, M.; Cammi, R.; Tomasi, J. *Chem. Phys.* **1998**, *238*, 153.
(58) Champagne, B.; Kirtman, B. *J. Chem. Phys.* **1999**, *108*, 6450.
(59) Kirtman, B.; Dykstra, C. E.; Champagne, B. *Chem. Phys. Lett.* **1999**, *305*, 132.
(60) Cammi, R.; Mennucci, B.; Tomasi, J. *J. Am. Chem. Soc.* **1998**, *120*, 8834.
(61) Marder, S. R.; Gorman, C. B.; Meyers, F.; Perry, J. W.; Bourhill, G.; Brédas, J. L.; Pierce, B. M. *Science* **1994**, *265*, 632.
(62) Marder, S. R.; Torruellas, W. E.; Blanchard-Desce, M.; Ricci, V.; Stegeman, G. I.; Gilmour, S.; Brédas, J. L.; Li, J.; Bublitz, G. U.; Boxer, S. G. *Science* **1997**, *276*, 1233.
(63) Yu, J.; Zerner, M. *J. Chem. Phys.* **1994**, *100*, 7487.
(64) Bartkowiak, W.; Lipinski, J. *Chem. Phys. Lett.* **1998**, *292*, 92.
(65) Zhu, W.; Jian, W. *Phys. Chem. Chem. Phys.* **1999**, *18*, 4169.